# Measuring Vehicle Roll, Tire Camber, and Camber Coefficient Using LIDAR

Alexander Brown, Sean Brennan
Department of Mechanical and Nuclear Engineering, Penn State University
University Park, Pennsylvania, USA
aab5009@psu.edu, sbrennan@psu.edu

**ABSTRACT**

This paper proposes a novel method for measuring suspension-induced vehicle roll and tire camber using a LIght Detection And Ranging (LIDAR) sensor. Kinematic relationships between vehicle roll and camber are developed and used to estimate a value for tire camber stiffness during a steady-state skidpad test. Finally, yaw rate measurements from a double lane change maneuver are compared to outputs from planar vehicle models with and without camber effects to assess camber's relative influence on the behavior of a particular test vehicle.

## 1. INTRODUCTION

Modern chassis control and state estimation methods make regular use of low-order planar single-track vehicle models. Elemental modifications to the traditional bicycle model equations, usually in the form of nonlinear tire models and/or weight transfer dynamics as in [1], add little complexity while adding significant fidelity to the model. As a result, model-based controllers [2] and vehicle state or parameter estimators [3] ,[4] are of low enough complexity that estimators and controllers may run in real time. Inclusion of camber effects, although a relatively minor contributor to overall vehicle behavior, could be useful in applications like [2] where transient vehicle performance is crucial. Model-based estimators like [4], seeking to identify tire properties, could also benefit from the inclusion of camber effects.

However, without access to a prohibitively expensive kinematics and compliance (K&C) measurement machine, experimental vehicle dynamicists have very few options when trying to determine the relationship between vehicle suspension movement (roll, pitch, and jounce) and effective wheel camber angle. Kinematic analysis of suspension geometry is one choice, but is fraught with uncertainty when employed on a real vehicle. Real vehicles are subject to bushing compliances, asymmetries, and linkage geometries that are fundamentally difficult to measure. In this paper, a relatively low-cost LIDAR sensor mounted rigidly to the vehicle sprung mass measures tire camber. Its fidelity is verified by comparing its estimate of relative vehicle roll with the measurement obtained from a defense-grade inertial navigation system (INS). Then, its measurement of front tire camber allows for estimation of tire camber coefficient during skid-pad tests.

## 2. TEST SETUP

The LIDAR system used in this study, a Hokuyo URG-04LX, has a 10 Hz update rate, a 240° swath, 0.35° angular resolution, and 1mm range resolution. The unit was mounted to the vehicle body on a rigid truss so that the scans could view the front-wheel attitude at the wheel center, as shown below.

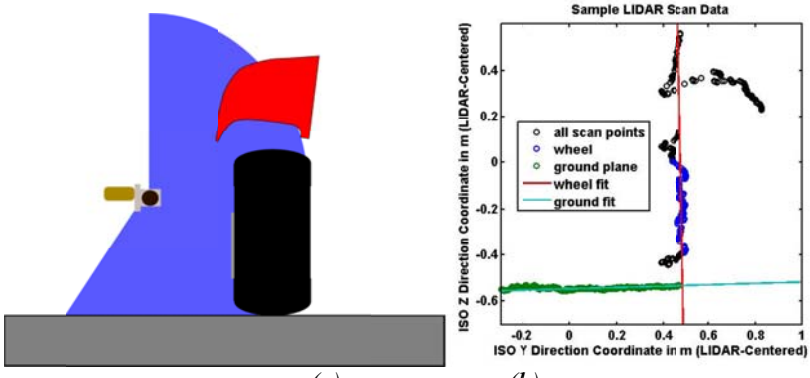


*(a)* *(b)*

*Figure 1. LIDAR Instrumentation Layout*

Figure 1(b) shows one time instant of the LIDAR scan, showing that system was able to measure the test vehicle's front wheel, the front tire sidewall, the ground outboard of the tire, and the front wheel well profile. This study was performed on a 1989 GMC 2500 equipped with a defense-grade INS/GPS system capable of 0.05 degree orientation accuracy in roll, pitch, and yaw. Vehicle roll angle was obtained directly by fitting a line to the ground-plane scan LIDAR points, and then by taking the inverse tangent of the fitted line's slope to obtain the relative roll angle of the vehicle with respect to ground (DC offset subtracted). Tire camber was obtained by simply examining the angle between the ground plane and the wheel plane.

## 4. LIDAR AS A ROLL AND CAMBER MEASUREMENT TOOL

While more expensive LIDAR sensors with higher update rates and lower noise levels exist, these units are, on the whole, much bulkier and require significantly more power than the unit used in this study. The URG-04LX uses USB power and is extremely light and easy to mount outboard of a vehicle body. A 10 Hz update rate may not be sufficient to acquire tire dynamics, but the roll and heave dynamics of interest for most passenger vehicles have cross-over frequencies in the 1-2 Hz range. Thus, the portion of camber dynamics which are kinematically determined by roll and bump of the tire should be measureable with the 0.1s sampling period. Figure 1 shows the LIDAR system mounted to two different vehicles—the first is the GMC 2500 used for the testing in this paper, and the second is the Penn State Formula SAE car.

*Figure 2: Physical mounting of the LIDAR sensor over the wheel plane for a GMC truck and F SAE vehicle.*

The Formula SAE car, while a good candidate for studying tire force vs. camber relationships due to its fully adjustable suspension, has significantly faster roll dynamics than a passenger vehicle (over 2.5hz), and has considerable tire compliance effects on camber that operate at around 10 Hz. Thus, a faster LIDAR system is advisable for a vehicle of this type if transient camber effects are to be measured.

Rather, the feasibility of using LIDAR for this purpose was assessed by measuring vehicle roll as compared to the high-accuracy INS mounted to the GMC test vehicle. When comparing LIDAR measured roll with measurements obtained from the INS system, the terrain-induced (static) roll angle was subtracted from the INS measurement so only roll due to vehicle suspension movement was considered. For this paper, a series of steady-state turning circles and a double lane change test were performed to examine steady-state and transient tire-ground interaction. Agreement during a lane change maneuver is shown in Figure 3.

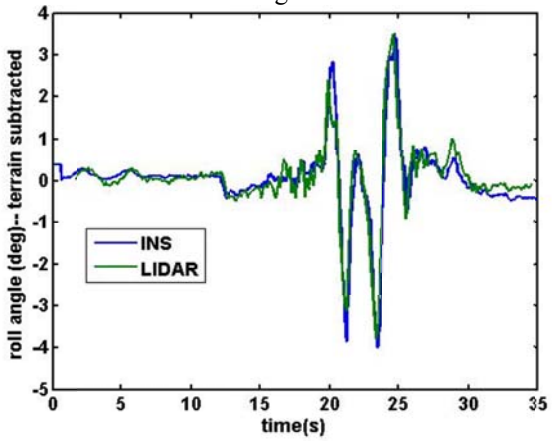


*(a)*

*Figure 3: Comparison of LIDAR and INS-measured roll measurements*

## 3. DETERMINATION OF SUSPENSION KINEMATICS

If the camber is assumed to vary nonlinearly with respect to vehicle roll, then a Taylor series approximation can be used to find behavior near the typical operating points. Analysis of the data shows that the trend is best fit via a cubic dependence from roll to camber angle. This fit is shown in Figure 4a

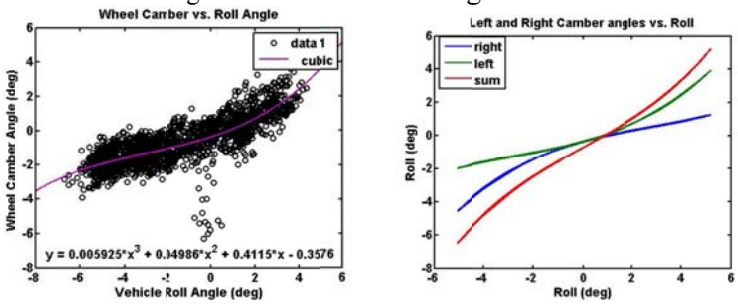


*(a)* *(b)*

*Figure 4: Camber versus. vehicle roll*

Although the LIDAR system was only measuring one tire (driver's side front), the same roll to camber relationship is assumed to hold for both the left and right front tires of the test vehicle due to right/left symmetry of the suspension design. With this assumption, one can infer the cumulative sum of these angles as shown in Figure 4b, which shows how the sum of the left and right cambers varies with vehicle roll angle. It is interesting to note that for this particular vehicle, camber is *always* "destructive," meaning that the camber thrust from the front tires always tends to counteract cornering force due to slip angle.

It is important to remember, too, that the camber data shown above includes effects from bushing compliances, steering, and roll-independent bump motion as well as effects from roll, and sensor noise effects. The disadvantage of this type of roll-to-camber fitting is that such effects are lumped together. The advantage, however, is that such effects are typically additive during normal driving maneuvers and thus, for prediction of vehicle dynamics, one would often want to determine the net effect of these terms, e.g. the understeer budget. Indeed, during skidpad tests, steer angles are small, bump motions are small due to a smooth track surface, and thus one can argue that camber might be idealized as a function of roll alone.

## 4. DETERMINATION OF CAMBER COEFFICIENT

The test vehicle used in this study, equipped with a double-wishbone suspension in the front and a solid axle in the rear, allows for the assumption of nearly zero camber change with respect to roll on the rear axle. For this reason, skid pad testing can provide a fairly accurate measure of rear cornering stiffness without taking camber into account. However, the front suspension does allow for measurable camber change with wheel travel, so the authors decided to focus on modeling this behavior to see if including camber effects on the front tires could improve low-order vehicle model accuracy.

### 4.1 Coordinate System

Because the standard convention for camber angle implies that positive camber results in the top of a tire leaning *away* from the vehicle centerline and negative camber results in the top of a tire leaning *towards* the vehicle centerline, this convention has mixed-handedness and is not suitable for the analysis of vehicle dynamics in one right-handed coordinate system. Using the ISO coordinate system standard, the camber and roll angles are redefined positive hereafter as shown below. Thus, compared to the prevailing convention for positive vs. negative camber, the passenger's side tire follows the convention while the driver's side tire does not

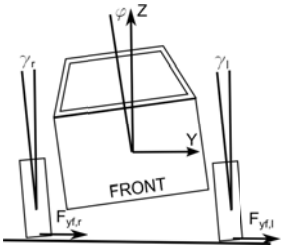


*Figure 5: Roll and Camber Angle Convention*

### 4.2 Tire Model

The results of this experiment are intended for implementation in low-order vehicle state models suitable for feedback control. Often, linear or saturated linear tire models are suitable for this application, as shown in [2]. Again assuming that the tires are operating with linear behavior, the lateral tire force on any tire can be written as in [6]:

$$F_y = F_y + F_\gamma = C_\propto \alpha + C_\gamma \gamma = F_v(C_s * \alpha + C_c * \gamma) \quad (1)$$

Where $C_\propto$ is cornering stiffness, $C_\gamma$ is camber stiffness, and $C_s$ and $C_c$ are cornering and camber coefficients. For the front axle in particular,

$$F_{yf,left} = C_{\propto f} \propto_f + C_{\gamma f}\gamma_{f,left} \quad (2a)$$

$$F_{yf,right} = C_{\propto f} \propto_f + C_{\gamma f}\gamma_{f,right} \quad (2b)$$

$$F_{yf,total} = 2C_{\propto f} \propto_f + 2C_{\gamma f}(\gamma_{f,right} + \gamma_{f,left}) \quad (2c)$$

It is here that some critical assumptions must be made to simplify the analysis. First of all, $\alpha_f$ and $C_{\alpha f}$ are assumed constant between the right and left wheels; in [6], Dixon writes a linear approximation for cornering *coefficient* as follows.

$$C_s = C_{s0}\left[1 + k_1\left(1 - \frac{F_v}{F_{v0}}\right)\right];\ k_1 \cong 0.6 \quad (3)$$

Where $k_1$ is the sensitivity of cornering coefficient to normal tire load. Assuming that both camber and cornering coefficients vary this way enables the additional assumption that left and right tire forces can be lumped together because changes in cornering stiffness due to left vs. right lateral load transfer are cancelled out.

### 4.3 Test and Analysis Procedure

To analyze tire forces, the vehicle is driven at or near steady state around a circular skid pad at slowly increasing velocity, and then the velocity is slowly decreased back to zero. This experiment is repeated for a clockwise and a counterclockwise circle. The vehicle's INS system measures slip angle, roll, and lateral acceleration, while the LIDAR system measures camber angle. Because the vehicle experiences very little yaw acceleration, planar equations governing front tire force reduce to:

$$F_{yf,r} + F_{yf,l} = \frac{m*b}{L} * a_y = 2C_{\propto f} \propto_f + 2C_{\gamma f}(\gamma_{f,right} + \gamma_{f,left}) \quad (4)$$

Where $a_y$ is the lateral acceleration at the vehicle CG, m is the vehicle mass, b is the distance from the vehicle CG to the rear axle, and L is the vehicle wheelbase. This tire force can be plotted directly as a function of measured slip angle—a first-order fit in the linear region of the tires' behavior yields a cornering stiffness value if tire force variation with camber is ignored. Plots outlining this method are shown below in Figure 6.

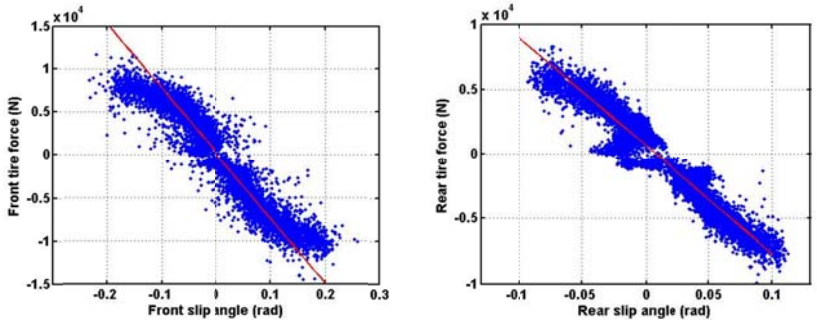


*Figure 6: Front (left) and Rear (right) slip angles versus force for steady turns.*

For the rear axle on the test vehicle in question, the cornering stiffness value above is considered to be equal to the slope of the lateral force vs. slip angle plot, since camber variation with roll is negligible for a solid axle suspension. The slope of the same plot for the front axle is more complicated, since camber effects are present.

At first glance, it might seem prudent to fit a plane to a 3-dimensional plot of $F_{yf}$ vs. total front camber angle and slip angle in order to obtain camber and cornering stiffnesses. The problem with this approach is that *at steady state,* the roll angle is nearly linearly related to lateral acceleration, which means that lateral acceleration and camber will

also have a strong functional relationship. In fact, for a steady state skidpad test, we can approximate this relationship as a linear equation.

$$(\gamma_l + \gamma_r) = \gamma = K_{a\gamma}\gamma \tag{5}$$

Thus, due to the absence of sufficient linear independence, cornering and amber stiffness for the front axle *cannot* be determined independently by examining front tire force (a direct function of lateral acceleration and vehicle measurements), front camber, and front slip angle alone. Figure 7 below shows the validity of equation (5) for the skid pad test performed. Net camber angle $\gamma$ was obtained by using the cubic fit for camber vs. roll outlined above.

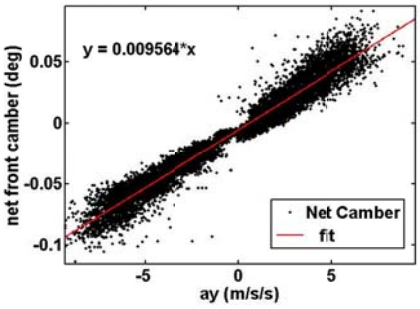


*Figure 7: Lateral acceleration versus measured camber.*

The results suggest that separating camber and cornering stiffness is impossible without additional information. However, if one uses the relationship between vertical load and cornering coefficient given in equation (3) along with the knowledge that the rear axle of this particular test vehicle experiences no camber gain with suspension movement, one can solve for an expected value of front cornering stiffness, $C_{\alpha f}^{*}$ using on [6]'s recommendation for load sensitivity and the value for rear cornering stiffness obtained from Figure 6 (right). Then, rewriting equation (4) in combination with equation (5),

$$\left[\frac{m*b}{L} + 2C_{\gamma f}K_{a\gamma}\right] * a_y = 2C_{\propto f} * \propto_f \tag{6}$$

Therefore, upon rearrangement, an effective camber stiffness for the front tires can be obtained from the slope of Figure 6 (left), which shows the relationship between total front tire force and slip angle. If the slope of this plot is $K_{\alpha f}$, then camber stiffness for the front tires can be approximated as

$$2C_{\gamma f} = \frac{m*b}{LK_{a\gamma}}\left(1 - \frac{2C_{\alpha f}^{*}}{2K_{\alpha f}}\right) \tag{7}$$

In essence, given the ratio of front cornering stiffness $2C_{\alpha f}^{*}$ to the slope obtained by plotting steady-state tire forces vs. slip, or $K_{\alpha f}$, along with the steady-state relationship between lateral acceleration and camber, camber stiffness can be obtained. Values obtained for camber stiffness are higher than those predicted by Dixon in [6], where he posited that camber stiffness is usually around 5% of cornering stiffness for radial tires. Values obtained for camber stiffness in this experiment were closer to 25% of the expected front cornering stiffness calculated via equation (3). It is possible that more precise values for load sensitivity could change these results, but the importance of having a contribution to tire force from camber angle extends well beyond steady-state cornering, as discussed in the next section.

## 5. INTEGRATION OF CAMBER EFFECTS INTO VEHICLE MODEL

Adding simple kinematic relationships between roll and tire camber to low-order models adds little complexity, but could have positive effects on accuracy. Inclusion of camber effects in a dynamic vehicle model have the potential to improve matches between models and data during transient maneuvers, when equation (5) relating camber to lateral acceleration does not hold. In transient maneuvers, the vehicle body is often out of phase with the inertial forces acting on the vehicle CG, which implies that camber forces may be either constructive or destructive, depending on the instantaneous direction of vehicle roll and the direction of vehicle acceleration. Figure 8 below shows a comparison between data collected during a lane change maneuver and two versions of the all-integrator form of the planar bicycle model—one including camber effects (via measured roll angle as an input), and one neglecting them.

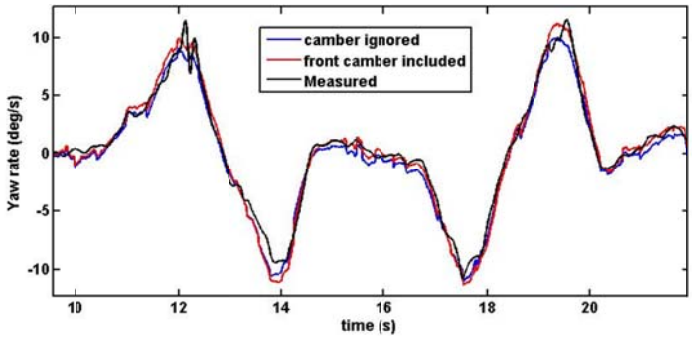


*Figure 8: Lane change maneuver measurements versus models with and without camber effects.*

The difference between the match for each model is relatively minor, which can be expected, since camber stiffness is a relatively small contributor to the overall eigenvalues of the planar vehicle model in yaw. However, the vehicle does seem to achieve yaw rates higher than those predicted by the planar bicycle model alone, and it is possible that this is because roll and lateral force demand are out of phase during a direction change, creating constructive camber thrust. Further, one can observe that inclusion of camber measurements enables higher-frequency motion to be captured by the model prediction, even with a low-order vehicle model. More detailed analysis of this phenomenon is necessary and planned for future work.

## 6. CONCLUSIONS AND FUTURE WORK

A new method for measuring camber and its relationship to roll angle was introduced. Camber and vehicle roll data were collected using a LIDAR sensor and used for experimentally determining the suspension kinematics of a test vehicle with no prior knowledge of vehicle dimensions or setup. Then, a method was proposed to determine tire camber stiffness using these kinematic relationships and a steady state skidpad test. A linear tire model including camber effects was investigated to improve model agreement between collected and simulated vehicle yaw rate during a transient maneuver.

While the proposed method only applies to a vehicle with a solid rear axle and an independent front suspension, testing at various tire normal loads, static camber values and vehicle weight distributions could strengthen results for camber stiffness. The authors believe that adding camber effects to low-order models could be very useful for feedback control and autonomous vehicle applications where a simple, analytical model is necessary for real-time vehicle guidance. Future work includes investigating the effect of including the obtained values for camber stiffness in a third-order linear roll model, especially in the frequency domain. The correlation frequency response analysis of a camber-equipped vehicle model may provide valuable information about whether camber plays a significant role in vehicle behavior in certain regions of the frequency spectrum.

**References**

[1] A. Rucco, G. Notarstefano, and J. Hauser: *Dynamics exploration of a single-track rigid car model with load transfer*, IEEE Conference on Decision and Control, 4934 – 4939, 2010

[2] H. Zhou and Z. Liu: *Design of Vehicle Yaw Stability Controller Based on Model Predictive Control*, IEEE Intelligent Vehicles Symposium, 802-807, 2009

[3] L. R. Ray, *Nonlinear tyre force estimation and road friction identification: Simulation and experiments,* Automatica, vol. 33, no. 10, 1819–1833, 1997.

[4] W. Cho et al.*: Estimation of Tire Forces for Application to Vehicle Stability Control* , IEEE Transactions on Vehicular Technology, Volume 59, Issue 2, 638-649, 2010

[5] Gillespie, *Fundamentals of Vehicle Dynamics*, SAE Press, 1992

[6] Dixon, *Tires, Suspension, and Handling,* SAE Press, 1997